Article

Not peer-reviewed version

Tests of the Tethered Class C3 Hexacopter in Maritime Conditions on the Landing Pad of a Ferry

Cezary Kownacki *, Leszek Ambroziak, Maciej Ciężkowski, Adam Wolniakowski, Sławomir Romaniuk, Zbigniew Kulesza *, Arkadiusz Bożko, Daniel Ołdziej

Posted Date: 4 July 2023

doi: 10.20944/preprints202307.0217.v1

Keywords: tethered multicopter; hexacopter; precision landing; moving landing pad; maritime conditions; tether unwinder

Article

Tests of the Tethered Class C3 Hexacopter in Maritime Conditions on the Helipad of a Ferry

Cezary Kownacki [1], Leszek Ambroziak [1], Maciej Ciężkowski [2], Adam Wolniakowski [2], Sławomir Romaniuk [2], Zbigniew Kulesza [2,*], Arkadiusz Bożko [1] and Daniel Ołdziej [1]

[1] Department of Robotics and Mechatronics, Faculty of Mechanical Engineering, Bialystok University of Technology, Wiejska 45C, 15-351 Bialystok, Poland; c.kownacki@pb.edu.pl (C.K.); l.ambroziak@pb.edu.pl (L.A.);arekbozko@gmail.com (A.B.); d.oldziej@pb.edu.pl (D.O.)

[2] Department of Automatic Control and Robotics, Faculty of Electrical Engineering, Bialystok University of Technology, Wiejska 45D, 15-351 Bialystok, Poland; m.ciezkowski@pb.edu.pl (M.C.); a.wolniakowski@pb.edu.pl (A.W.); s.romaniuk@pb.edu.pl (S.R.)

* Correspondence: z.kulesza@pb.edu.pl; Tel.: +48-797-990-780

Abstract: Various UAV applications, especially those based on reconnaissance and observation missions, often require an unlimited time of flight. This is possible only when a UAV is being continuously power supplied from the ground power source, and that is why tethered UAV systems were developed. Tethered UAV systems are based on multicopters which can hover above the landing pad, or track its position in the case it is movable. The presented research is about the development of a large C3 class hexacopter having a maximal payload of about 1 kg, and takeoff mass of 16 kg, which was tested in maritime conditions during the ferry's cruise. The main purpose of the hexacopter is the continuous observation of the area ahead of a vessel to detect and localize obstacles in the water. During experimental tests critical phases of flight were identified, the AC-DC power supply unit as well as the power cord unwinder were tested, and the power taken by six BLDC motors was registered. The obtained results can be useful in future work on tethered UAV systems used in windy maritime conditions.

Keywords: tethered hexacopter; precision tracking & landing; moving helipad; maritime conditions, tether unwinder

1. Introduction

The usage of UAVs in vessel-based missions has been highlighted significantly due to their ability to provide an effective platform for numerous purposes. With enhancements made to aerial vehicles' technology and sensor miniaturization, UAVs have emerged as significant contributors towards maritime activities. These unmanned planes furnish superior situational awareness alongside seamless collection capabilities of data that make it much more affordable than conventional techniques.

The most common applications of UAV systems are focused chiefly on observation and reconnaissance missions [1]. It is obvious that advanced vision systems and flights at a hundred meters above the ground significantly increase the range of visual observation. It can be proven by drone usage in modern wars, where identifying enemy positions is crucial in a successful strike [2]. Drones and their vision systems are excellent tools to monitor the borders of countries [3] or forests to protect against fires [4]. Another possibility of UAV observations, which can be a challenge, is to recognize and localize objects on water surface that can be dangerous for vessel's structure [5,6]. It is especially important if future vessels are unmanned, and a great number of lost containers are in the seas. To prevent unexpected collisions, monitoring should constantly operate, with a range of view to perform avoidance maneuvers. This could be possible with a UAV which is continuously power supplied from the deck of the vessel and with the flight altitude at least 50 meters. Therefore, the current paper focuses on such kind of the UAV, i.e. on a tethered multicopter whose payload is sufficient to mount advanced cameras. This paper presents flight tests of the tethered multicopter in

 doi:10.20944/preprints202307.0217.v1

maritime conditions in a standard cruise of the ferry "Wolin" over the Baltic Sea. Test results which are a composition of the observations and recorded flight parameters, can be used to identify potential issues of UAV usage in maritime conditions on a deck of a vessel, especially related to gusts and turbulences of the wind over the helipad. The paper presents ultimate results of the UAV operation in sea conditions. The UAV was developed based on the conclusions and invaluable experience from the tests in quasi-real conditions carried out on the lake, which were presented in [7].

The article consists of six sections and the first one is the introduction with a subsection, where there is a review of current advances in tethered UAV systems. The second one contains a detailed description of the designed tethered hexacopter system, including separate subsections sequentially about the tethered hexacopter, the power cord unwinder, the equipment required for tracking of the helipad position, and the UWB (Ultra Wide-Band) positioning system. In the third section, experimental tests performed flight missions, and weather conditions during the ferry cruise over the Baltic Sea are presented. The last two sections are dedicated respectively to discussion on results and final conclusions.

1.1. Current Advances in Related Research

Unmanned Aerial Vehicles (UAVs) are a transformative technology showing tremendous promise for several sectors, one of which is the maritime industry. A closer analysis reveals a range of perks the utilization of these vehicles offers: efficient retrieval of data streams; advanced surveillance standards preserving public safety while substantially cutting costs for operators. Nevertheless, many impediments need overcoming before fully deploying this budding technology in mission-critical tasks involving vessels: regulations on multiple levels, limited technical capacities, and adverse operating circumstances all pose formidable challenges. In order to achieve the maximum potential from the marine-based application scenarios, it is essential that related issues are addressed comprehensively.

Over the course of several consecutive years, numerous research teams have dedicated their efforts to overcome various challenges associated with operating UAVs in maritime conditions. The constraints imposed by limited resources such as specialists, work hours, and available deck space on ships and boats pose major challenges. Consequently, engineers are compelled to develop autonomous systems that are both maintenance-free and reliable. Nevertheless, the creation of fully autonomous solutions that can be used in commercial applications, proves to be exceedingly expensive and financially unfeasible for many companies and research institutions. As a result, progress is made incrementally within specific domains of expertise.

One of the main applications of the UAV in maritime conditions is photogrammetry, which is a technique to create detailed and accurate 3D maps using the aerial photography. Development and evolution of the UAV in terms of operational costs and reliability strongly increased the accessibility and efficiency of photogrammetry [8]. This is even more important for the seas due to the increased costs and risks of manned flights. UAVs are easy to deploy and offer a reasonably high spatial resolution and accuracy. Determination of the high-density models of the sea floor utilizing the LIDAR data acquired by UAV is presented in [9]. Data resolution is a vital parameter in various aerial imaging tasks. When faced with limitations due to small size and weight of the measuring devices, artificial intelligence based enhancement techniques can be employed to overcome these limitations. In a research study discussed in [10] the set of super-resolution (SR) methods has been explored, including those that leverage the concept of Generative Adversarial Networks (GANs). These techniques aim to enhance the acquired information and improve the resolution of aerial imagery, enabling more detailed and accurate analysis. By leveraging advanced algorithms and deep learning approaches, the SR methods offer potential solutions to enhance the quality and level of detail in aerial images, thereby expanding their applicability in different domains.

SAR (Search And Rescue) missions are another prominent field where UAVs find wide utilization. Specifically, VTOL (Vertical Take-Off and Landing) platforms are commonly employed for conducting extensive marine surveillance with a focus on wide-area coverage and continuous monitoring.

 doi:10.20944/preprints202307.0217.v1

Numerous systems have been specifically designed for this purpose, as highlighted in [11,12]. Additionally, the development of various UAV systems takes into consideration the requirements and challenges associated with SAR missions, as referenced in [13]. This underscores the significance of UAV technology in enhancing search and rescue operations, particularly in maritime environments.

The overall performance of the UAV in various tasks is not only dependent on advancements in data acquisition and processing for specific applications but also relies heavily on the UAV's parameters and its ability to comply with system commands. These parameters include characteristics such as flight stability, maneuverability, payload capacity, and endurance, which directly impact the UAV's effectiveness in executing tasks. Accurate and precise localization plays a crucial role in mostly autonomously operated robotic systems. While conditions meet on the seas typically involve fewer obstacles that block the GNSS satellite signals, in specific they are met at just over the line dividing the sea from the sky, the weather conditions which often can't be properly forecasted at sea can disrupt satellite systems. As a result, traditional navigation methods of the drones become less useful due to limited reliability, particularly when systems based on optical flow exhibit reduced accuracy over the water's surface. To address these challenges, many researches in the topic of UAV applications have leveraged the benefits of systems utilizing the Real Time Kinematic (RTK) method. Lewicka et al. [14] highlighted the importance of accurate and precise tracking of the trajectory using the GNSS-RTK in order to collect and localize a series of many aerial images. Likewise, in a separate investigation documented in [15], the application of GNSS-RTK to perform an data fusion in terms of geospatial applications was introduced. When coastal environments is considered, accurate and precise localization has been employed for qualitative spatial analysis, integrating techniques such as terrestrial laser scanning, photogrammetry, and historical bathymetric map data and bathymetric surveying. Despite the potential for significant drift in the global position measurements due to the RTK station being situated on a landing pad moving in relation to global coordinate system, correcting signal disruptions significantly enhances the accuracy of relative positioning. Overall, the utilization of RTK systems in UAV operations addresses the challenges of precise localization, compensating for the limitations posed by maritime conditions and ensuring more accurate and reliable positioning. This enables the successful integration of various geospatial techniques, facilitating high-quality data analysis and enhancing the overall performance of UAVs in maritime environments. Besides relying on GNSS systems for global range navigation and system basing on video data for precise landing pad approach, systems from a level in between the above mentioned that utilize radio frequencies play a vital role in facilitating various UAV operations. Various commonly-spotted and widely used systems for wireless data transfer such as Wi-Fi, Bluetooth, and others are commonly employed for positioning purpose, each with their own constraints and effectiveness. Yang and Yang conducted a comprehensive review of this topic in their study [16]. Their research delves into the utilization of different wireless data transfer technologies, exploring their capabilities, limitations, and applications within the UAV domain. By examining the effectiveness and practicality of these systems, their work provides valuable insights for optimizing data transmission and communication in UAV operations.

Usually, in UAV missions two crucial moments can be identified: take-off of the UAV and landing. The Surface vehicles have their dynamic characteristics that are influenced by several factors, including their type, scale, weight, inertia and prevailing weather conditions. During a most-common mission scenario, a vessel experiences various types of motion that affect its position and orientation in the marine environment. These motions can be categorized into translational movement, vertical movement, and oscillations in the roll angle. To ensure mission success, the UAV system must be resilient to these disturbances. Extensive analysis of the complexity associated with landing on moving and rocking platforms has been conducted in a comprehensive study discussed in [17]. The proposed solution not only encompasses control algorithms and software but also introduces a leaning gear with a mechanical self-adaptation as an integral component. Another study by Tang et al. [18] improved landing stability by implementing an tripod that can be adjusted. The proposed tripod includes omni wheels at the end of each arm. Furthermore, the study presented in [19] introduces a dedicated system

 doi:10.20944/preprints202307.0217.v1

designed specifically for landing on moving vessels, which can also be used to land on moving vehicles. In this particular approach, the burden of time and resources consuming calculations together an analysis of data is shifted to a ground station situated near the take-off and land place. This strategy aims to streamline the operation of the UAV by offloading computational tasks to a centralized system. By doing so, the UAV can focus on its primary objectives without being encumbered by extensive onboard processing requirements. The estimation of the relative position in these landing systems was achieved through sensor fusion using a stereo camera for vision system, fiducial markers to mark the object, and position estimation through the usage of Deep Neural Networks (DNN). Finaly the position was estimated using a Kalman filter that incorporated fusion of the data from the visual system and telemetry from the Internal Measurement Unit (IMU). To ensure adaptability, a finite state machine-based logic was implemented, allowing for trajectory adjustments based on qulatitative indicator of the tracking accuracy and the influence of ground effects.

The publication by Grlj et al. [20] provides a comprehensive review and analysis of the mobile landing platforms that were developed and presented in the literature. It delves into various aspects such as procedures of landing and take-off, accuracy and precision of position estimation, control algorithms, fundametal rules and algorithms for trajectory generation, as well as systems for autonomous docking. The study offers valuable insights and findings in these areas. In a similar vein, the implementation of visual positioning for the non-stationary landing pad was explored in [21], utilizing the Robotic Operating System framework. This approach shares similarities with the currently proposed solution, emphasizing the importance of visual cues for determining the relative position of the UAV in the USV (Unmanned Sea Vehicle) local coordinate system (or vice versa).

While vision systems are widely popular for relative positioning, alternative methods have also been investigated. In [22], a set of ultrasonic sensors was mounted on the USV to detect the presence of the multirotor over the landing pad. This approach demonstrates an alternative means of achieving relative positioning between the two robots. To facilitate coordinated navigation between the UAV and USV, a coupled navigation system was introduced in conjunction with a newly developed guide point generation algorithm. This system ensures the synchronized movement and enhances the overall efficiency and effectiveness of the mission. Through these research contributions, a deeper understanding of mobile landing platforms, their functionalities, and their interaction with UAVs and USVs has been achieved. These studies provide valuable insights for the development of robust and efficient systems for UAV and USV collaborations. The incorporation of a manipulator arm and docking terminal on a heterogeneous mobile landing pad was explored in [23]. The docking terminal features a socket on the bottom specifically designed to match the UAV configuration. Precise localization is achieved through the utilization of fiducial markers, ensuring accurate positioning during the docking process. The control system implemented in the study combines predictive, reactive, and optimal approaches to manage the landing and docking operations. This fusion of control strategies ensures efficient and reliable coordination between the UAV and the mobile landing pad. Aforementioned system exhibits a high degree of redundancy, facilitated by the extensive freedom of movement provided by robotic arms. The successful integration and cooperation of the UAV and the mobile landing pad results in a symbiotic relationship. The UAV wide field of view and aerial capabilities complement the wheeled vehicle high payload capacity, potentially serving as a charging station for the aerial robot. This effective collaboration maximizes the utilization of both platforms, unlocking their full potential in various applications.

The work of Palafox et al. [24] provided valuable insights into vision system-based tracking of the landing pad. Another notable study, referenced as [25], proposed the use of a tethered UAV. However, the main objective of the tethered UAV was not to serve as a power supply but rather to ascertain the position of the aerial untis in relation to ground units. Specific configuration of the loose tether was determined by observing different mechanical components, which in turn provided valuable insights into the positions of the robots in their respective local coordinate systems. In contrast, a rather unconventional approach was presented in [26], introducing Unmanned Surface

Preprints (www.preprints.org) | NOT PEER-REVIEWED | Posted: 4 July 2023 doi:10.20944/preprints202307.0217.v1

Vehicle (USV) utilizing a solar power which was designed specifically for recovering waterproof UAVs which were splashed down into the water with an intention. It is important to note that while this concept demonstrated effectiveness for such scenarios, its applicability to large-scale ocean vessels is limited. These various research endeavors contribute to the exploration and development of different techniques and platforms for visual tracking, relative position determination, and recovery of UAVs, showcasing the diverse strategies employed to address specific challenges in maritime operations.

2. Architecture of the Tethered Hexacopter System

An overview of the proposed tethered hexacopter system is presented in Figure 1. Two main components of the system are: the aerial part, i.e. the systems used on the hexacopter, and the water-based part, installed on the landing deck of a ferry. The diagram highlights the relationships and connections between subsystems, while detailed specifications are provided in subsequent chapters.

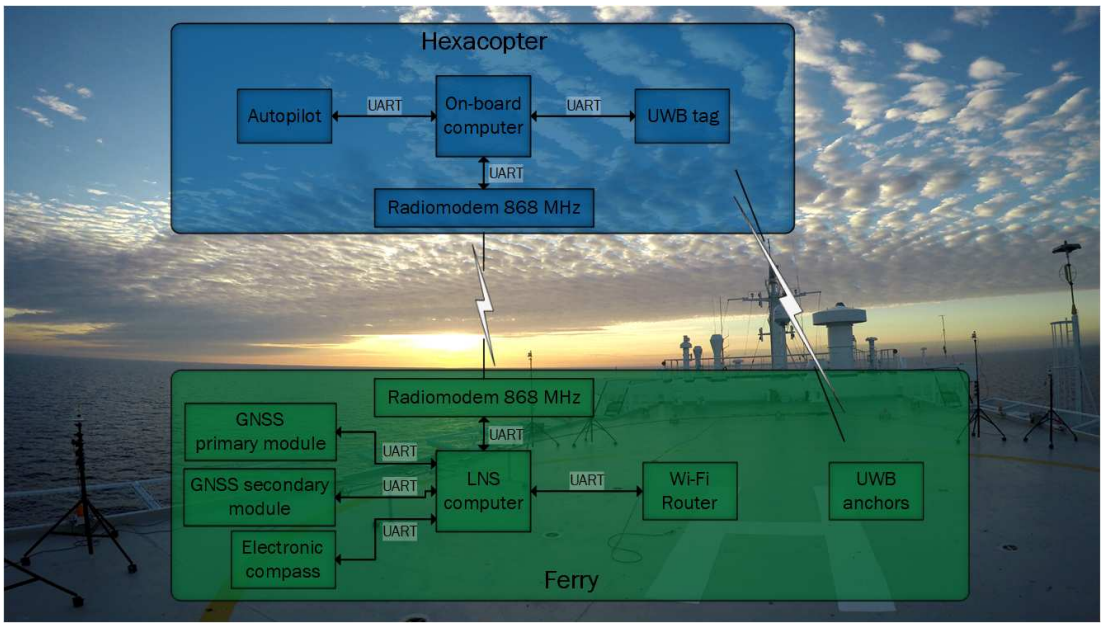

Figure 1. Overview diagram of the Tethered Hexacopter System.

2.1. Tethered Multicopter

The carrying platform of the proposed system is an unmanned aerial vehicle of the multi-rotor helicopter type. Analyzing the aspects of reliability and lifting capacity in the design phase, it was decided to use the hexarotor configuration. It is a good combination of drive redundancy and compact dimensions. The hexarotor is shown in Figure 2.

In Figure 2 the frame of the multicopter (Figure 2A), a single arm—one of the six (Figure 2B), the drive unit consisting of a propeller, the BLDC motor and the electronic speed controller (Figure 2C), converters power supply system (Figure 2D), the landing gear (Figure 2E) and the control system—the autopilot with the GNSS receiver (Figure 2F) are presented.

Characteristic for this unmanned aerial vehicle is the fact that it is powered by wire from the ship's deck. Electricity is transmitted via a special cable from a ground source to dedicated electricity converters on the board the UAV. In addition, the hexarotor has a battery buffer in the event of damage to the tether so that it is able to perform a quick but controlled landing. The weight of the helicopter, depending on the optoelectronic equipment and the length of the power cable, oscillates between 10.5-13.5 kg. The demand for electricity in the hover, depending on the prevailing weather conditions, is 1500-2000 W. At its peak, during the take-off phase and the fight against turbulence, the multi-rotor can consume up to 3.6 kW in peaks. The main parameters of the multi-rotor unmanned aerial vehicle are listed in Table 1.

Preprints (www.preprints.org) | NOT PEER-REVIEWED | Posted: 4 July 2023 doi:10.20944/preprints202307.0217.v1

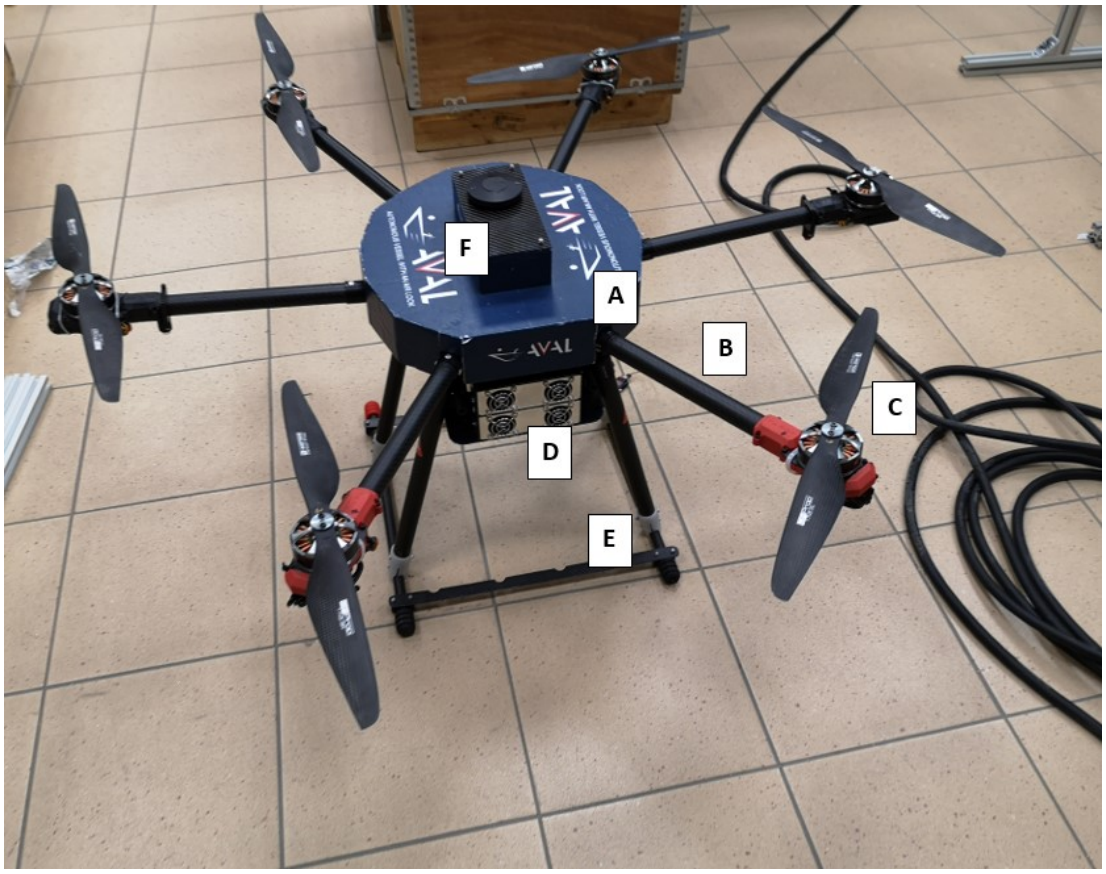

Figure 2. Multi-rotor in six-arm configuration.

Table 1. Multi-rotor basic characteristics

Parameter	Value
Dimension between opposite motors	960 mm
Wheelbase diameter (top view)	1400 mm
Max. single drive thrust	40 N
Max. take-off mass	13.5 kg
Payload	3 kg
Power type and source	Electric, tethered from ground (vessel)
Motor type	Brushless DC motor
Wind resistance	16.6 m/s
Flight duration	Unlimited*

* Depends only on the reliability of the power supply via the cable.

The hexacopter can be controlled manually from the level of the remote control apparatus and the pilot-operator, or automatically from the level of the computer, where then the man performs only a supervisory function. The unmanned aerial system (with other described below components) on the ferry "Wolin" helipad deck is shown in Figure 3.

2.2. Tether Unwinder

The design of the cord unwinder was a challenge because of the desired altitude of the flight mission and the hexacopter power consumption. To achieve a reasonable range of view for the onboard vision system, the flight altitude should not be less than 50 meters. Therefore, the total cord length must also be at least 50 meters. On the other hand, the six motors of the hexacopter consume about 3 kW of power. Hence, the weight of the power cord to be lifted by the hexacopter as payload is about 3.6 kg and. Note that, the power cord was specially selected for this application. To provide constant unwinding and winding speed, and to have power cord tension independent from the current length

Preprints (www.preprints.org) | NOT PEER-REVIEWED | Posted: 4 July 2023 doi:10.20944/preprints202307.0217.v1

of its unwound part, the cord must be wound evenly on the main roll. Thus, the structure of the power cord unwinder must meet these specifications. It is shown in Figure 4.

Figure 3. Tethered hexarotor with other UAS components on the ferry's top deck

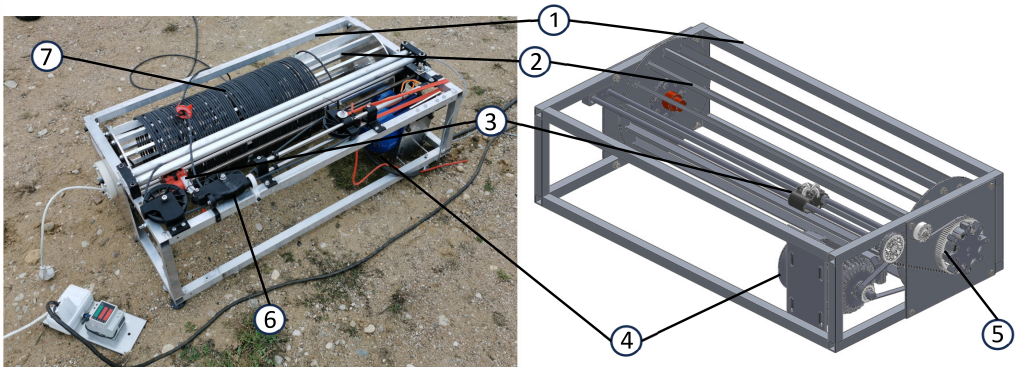

Figure 4. The structure of the power cord unwinder. 1 – frame, 2 – winding roll, 3 – guiding trolley with a tension sensor (potentiometer), 4 – AC asynchronous triple phase motor, 5 – belt transmissions, 6 – damper, 7 – 50 meters of power cord.

A guiding trolley ③ mounted on the screw, moves proportionally to the length of the unwound/wound power cord ⑦, in the way guaranteeing that the cord will be wound coil by coil on a single layer. It is crucial because 1 mm^2 wires of the power cord can be temporarily overloaded and must be cooled by the air. The openwork structure of the roll with the power cord helps with this. On the other hand, a power cord with 1.5 mm^2 wires would be too heavy. The roll ② with the power cord is driven through a belt transmission ⑤ by a triple-phase AC asynchronous motor ④ controlled by a single-phase inverter. A dancer roll on the guiding trolley end rotates a potentiometer which is connected to the inverter's speed input. The position of the potentiometer decides both the speed and direction of the roll rotation. A pulling spring rotates the potentiometer to the winding position of the cord with maximal speed. Applying the required tension to the dancer's roll moves the

Preprints (www.preprints.org) | NOT PEER-REVIEWED | Posted: 4 July 2023 doi:10.20944/preprints202307.0217.v1

potentiometer's slider to the neutral position and unwinding or winding stops. Too high tension moves the potentiometer slider to the unwinding position. This way, tension is applied to the power cord by the ascending or descending UAV and switches the unwinder between winding and unwinding to provide desired tension value. To reduce tension oscillations and secure the unwinder against sudden jerks of the power cord, a damper ⑥ is installed on the unwinder's frame ①.

2.3. Navigational equipment for landing pad position tracking

This chapter provides a description of the necessary navigational equipment to implement precision UAV navigation. These equipment include a landing pad navigation station, an on-board computer and an autopilot.

- Landing pad navigation station

The landing pad navigation station (LNS) serves as a command, measurement, and communication apparatus. Its primary functions include measuring navigation variables of the landing pad, managing unmanned aerial vehicle (UAV) flight, and exchanging data with the UAV's onboard computer through a radio link. The navigation variables measured by the LNS include the landing pad's current position in the WGS-84 reference system, velocity and heading. The LNS is responsible for transmitting take-off and landing directives to the UAV and exchanging navigation data with the UAV's onboard computer.

The landing pad navigation station is presented in Figure 5. The station comprises the main computer (see ① in Figure 5), two GNSS modules with antennas (the primary ② and the secondary ③), the electronic compass ④, and the radio module ⑥ for communication between the LNS and the UAV. The station also features the Wi-Fi router ⑤ to establish a service or supervisory connection with the main computer. The structural framework of the LNS is constructed using aluminum profiles connected by mounting brackets and captive nuts. Figure 5 presents the key dimensions of the station.

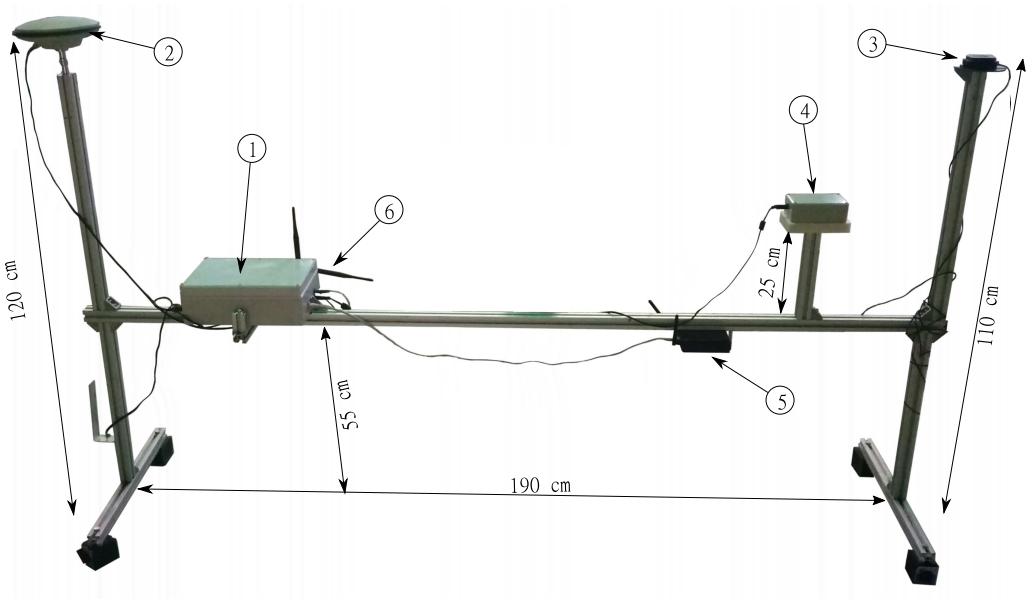

Figure 5. Landing pad navigation station: 1 – main computer, 2,3 – GNSS modules with antenna, 4 – electronic compass, 5 – WiFi router, 6 – radio module.

All measuring devices within the LNS are linked to the Computing Unit located inside the main computer ①. The hardware platform of the Computing Unit is an embedded computer Kontron [27]. The navigation system is controlled by a dedicated application which runs on the Computing Unit. This application acts as a UAV Ground Control Station (GCS) software, responsible for collecting measurement data from the station and managing the entire aircraft flight.

Preprints (www.preprints.org) | NOT PEER-REVIEWED | Posted: 4 July 2023 doi:10.20944/preprints202307.0217.v1

The primary GNSS module determines the position and velocity of the landing pad in the WGS-84 reference system. On the other hand, the secondary GNSS module calculates the heading of the landing pad by analyzing the positions of both primary and secondary GNSS module antennas. Spherical trigonometric relationships are used to compute the heading accurately within approximately $\pm 1°$. To achieve this accuracy, the secondary GNSS operates in the RTK (Real-Time Kinematic) moving base mode. The GNSS modules are interconnected via UART - the primary GNSS transmits RTCM corrections to the second one. Furthermore, the separation distance between the GNSS antennas must exceed 1 meter [28]. The RTK functionality is delivered by GNSS U-blox modules [28]. To ensure system reliability when the RTK mode is unavailable, such as during adverse weather conditions, the navigation station includes the electronic compass [29].

- On-board computer

The onboard computer serves as a crucial component, enabling the execution of the positioning and navigation of the UAV. It is tasked with obtaining and filtering the accurate relative positioning data based on the UAV and the base station GNSS coordinates. This estimate is further enhanced by including position information from the local positioning system (the UWB system). In order to provide this functionality, the onboard computer services the UWB tag mounted on the airframe. The computer operates a ROS-based framework that uses a Mavlink bridge to forward the messages between the autopilot and the ground control station.

The Odroid on-board computer and the Pixhawk autopilot communicate over the UART protocol. To establish a downstream connection with the ground station, a radio-link is employed, utilizing the serial protocol. Additionally, an optional Wi-Fi connection is available to facilitate diagnostics and system performance testing. The UWB receiver is connected with the on-board computer through the USB.

The ROS framework used to implement the positioning and navigational functionalities consists of several components. The diagram of these components and their interactions is shown in Figure 6.

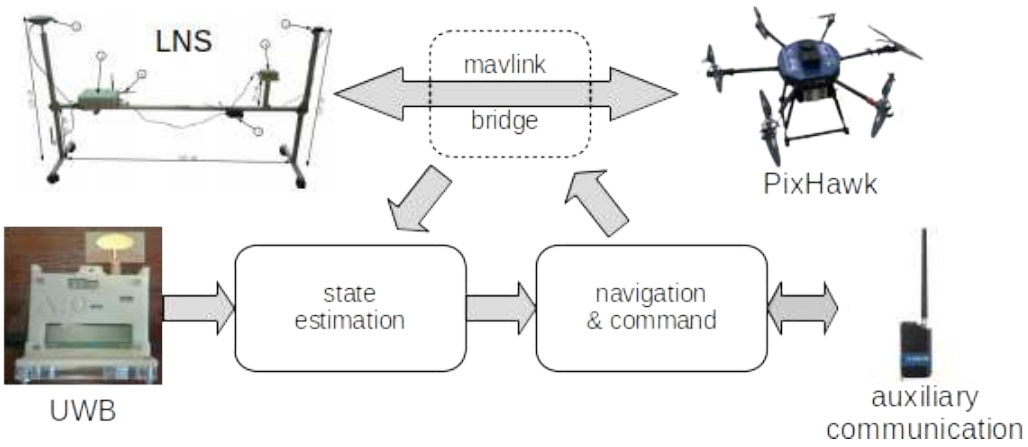

Figure 6. Diagram of the on-board computer framework.

The components can be briefly described as follows. The *mavlink bridge* component forwards the messages sent upstream from the LNS to the autopilot and extracts the information about the base station position and the desired UAV position from the additional custom packets inserted into the stream. The bridge also forwards the downstream packets from the autopilot to the LNS and extracts the state information of the UAV. The state information, including the position estimate obtained through the *UWB* component is processed in the *state estimation* component, where the precise position of the UAV wrt. the base station is calculated. The state estimate is further used by the *navigation and command* component to compute the desired steering of the UAV. Additional *auxilliary communication* component is also available to process diagnostic information and logging.

Preprints (www.preprints.org) | NOT PEER-REVIEWED | Posted: 4 July 2023 doi:10.20944/preprints202307.0217.v1

- Autopilot

Although the autopilot directly controls the flight of the UAV by managing motors and aileron positions, the communication between the LNS and the UAV does not occur directly with the autopilot itself. Instead, the LNS Computing Unit communicates with the UAV's on-board computer. The on-board computer plays a crucial role in integrating data from the positioning system and establishing communication with the autopilot. Essentially, the LNS station transmits take-off and landing orders, directly to the autopilot through the UAV's on-board computer. Meanwhile, the UAV's on-board computer is responsible for determining the tracking error between the UAV's actual position and the estimated position provided by the LNS. This information, including the estimated position and velocity from the LNS, is then relayed to the control loop of the autopilot.

The autopilot that manages the drone's operation is the Pixhawk PX4 [30]. To regulate the altitude and heading of the UAV, the standard control algorithm implemented in the autopilot firmware is utilized. However, achieving control over the horizontal position (x, y) requires making adjustments to the flight control code. In this case, the control loop for the horizontal position of the drone takes into account both the relative position error between the UAV and the LNS and the horizontal velocity of the landing pad.

The altered control framework of the PX4 autopilot, with the relevant modifications highlighted in red color and blue is depicted in Figure 7. The key distinction from the original architecture is that the desired horizontal speed $\vec{V}_{U_D}$ of the UAV is directly fed into the *Velocity Control* block.

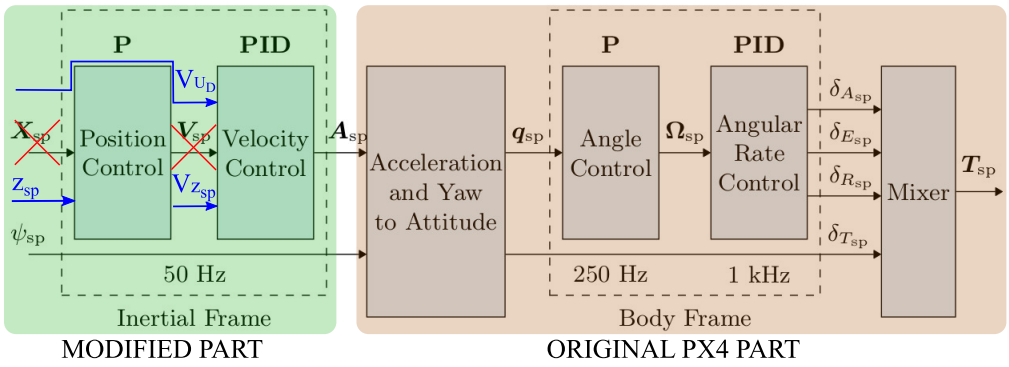

Figure 7. Modified autopilot control architecture [31].

2.4. UWB Positioning System

The local positioning system is developed utilizing the Ultra Wide Band (UWB) technology, serving as an integral component within the relative positioning algorithm. For estimating position accurately, this system employs a technique known as lateration that relies on measuring distances. It uses two types of ranging devices: anchors placed stationary at the landing pad and tags mounted on unmanned aerial vehicles (UAVs). By integrating these distance measurements with established anchor positions precise calculations can be made to determine each tags' specific location.

To address the specific requirements of fast-moving flying objects and the integration of positioning systems, a specialized structure of the positioning algorithm is implemented. Three distinct stages can be distinguished in the aforementioned algorithm, as illustrated in Figure 8.

One of the primary concerns in the mentioned application revolves around the possibility of the UAV exceeding the serviceable range of the measurement in the UWB devices. In such cases, some or all of the distance measurements may become unavailable. Another issue arises when the distance between the measuring devices gets close to the maximum range that can be measured, resulting in intermittent distance measurements and highly distorted values. Furthermore, obstacles like cables, trees, the UAV itself, humans, or terrain can obstruct the radio signal, affecting distance measurements. To overcome these challenges, the UWB-based positioning algorithm incorporates an evaluation of the distance quality in its initial stage.

Preprints (www.preprints.org) | NOT PEER-REVIEWED | Posted: 4 July 2023 doi:10.20944/preprints202307.0217.v1

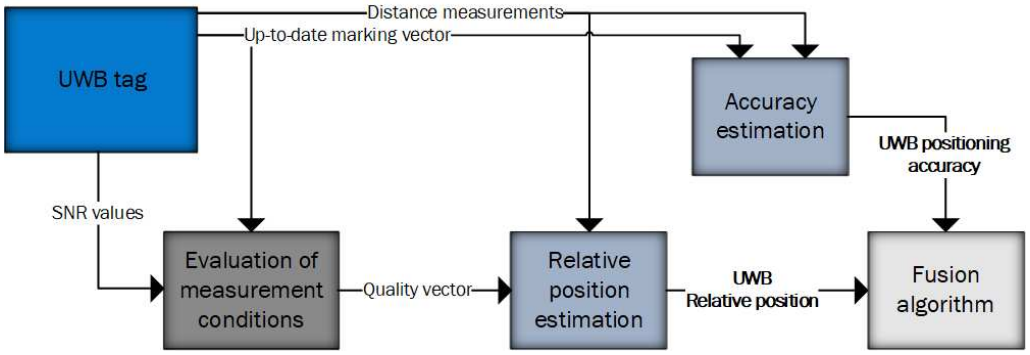

Figure 8. Dataflow of the adaptive UWB positioning algorithm [7].

When the first stage finishes, every distance measurement is classified into one of three categories: measurement taken without any disturbances, a measurement affected by poor conditions, or a non-usable measurement. The quality of each measurement is assessed by utilizing the update flag and the signal-to-noise ratio (SNR) value, which are transmitted within the data frame by the UWB modules used in the positioning system.

During the initial step, the update flag is carefully analyzed. In the update flag, a dedicated bit is assigned to each measurement, with a value of 0 indicating the inability to obtain the measurement between a specific anchor and tag. Subsequently, the SNR parameter is evaluated. Measurements captured under unfavorable conditions are determined by evaluating the ratio between the signal-to-noise ratio (SNR) and the distance. If this ratio falls below a predefined threshold, the measurement is considered to have been taken in less-than-optimal conditions. Measurements with an SNR value lower than another threshold are considered non-usable. During testing, the threshold of the SNR was defined at -18 dBm. It is important to note that when the SNR value decreases below -20 dBm, the measurements tend to be inconsistent and significantly less accurate [32] and [33]. To address this phenomenon, the threshold was intentionally set 2 dBm higher than the observed boundary. This adjustment helps mitigate the impact of the discontinuity and accuracy issues caused by low SNR values. By setting the threshold at -18 dBm, positioning ranges exceeding 35 m can be achieved while simultanously meeting the primary objective to prevent substantial error spikes in the results, as they have the potential to compromise flight stability.

The second stage of the algorithm heavily relies on the evaluated distance measurements, which serve as vital inputs for the robust Extended Kalman Filter. This filter plays a crucial role in processing and incorporating the measurements to estimate the tag's coordinates accurately.This adaptive filter can effectively handle varying numbers of inputs in subsequent steps, ensuring reliable estimation of the tag's coordinates. For reliable estimation of the tag's coordinates, a minimum of four usable distance measurements is required.

During the final stage, the accuracy of the position calculation is evaluated. The evaluation process takes into careful consideration various factors, including the number of accurate measurements, the quality and reliability of those measurements, and the distance between the anchor and the tag. These critical aspects are thoroughly assessed to ensure the validity and effectiveness of the evaluation. The adaptive UWB-based positioning system provides the estimation of the relative position of the UAV, along with an assessment of its accuracy, to the algorithm performing an integration of the data provided from different measurement systems in order to output an final UAV position in relation to the position of landing pad. This approach ensures that UWB measurements are excluded during the integration stage if the UWB system is unable to estimate the UAV's position. By considering the reliability of the UWB system's estimations, the integration stage selectively incorporates measurements from other reliable positioning systems. This exclusion helps maintain the accuracy and integrity of the integrated position estimation by avoiding the inclusion of potentially unreliable or erroneous data. As a result, the integration algorithm can generate more robust and

Preprints (www.preprints.org) | NOT PEER-REVIEWED | Posted: 4 July 2023 doi:10.20944/preprints202307.0217.v1

trustworthy estimates of the UAV's position by leveraging the most reliable and accurate sensor information available.

3. Tests on the ferry in real maritime conditions

The tests were carried out in the winter season in February. They took place on a real facility—the ferry "Wolin" travelling from Swinoujscie (Poland) to Trelleborg (Sweden) according to its daily schedule. During the cruise, despite the fact that it lasts about 7 hours, the convenient window for the test is very narrow due to e.g. leaving the port and getting to the port, passing wind farms or forbidden zones, bad weather, dusk—where flight tests should not be set. During the window of possible tests, additional calibrations or parameter changes often had to be performed, which additionally took up valuable time. Finally, on a given day, 6 flights of different duration and altitude were made. The hexarotor in flight above the ferry deck in real sea conditions is shown in Figure 9. The ambient conditions during the aerial mission were as follows:

- average temperature: 9 °C,
- relative wind speed: 11-18 m/s,
- gusts of wind: up to 22 m/s,
- cloudiness: 80 %,
- humidity: 74 %.

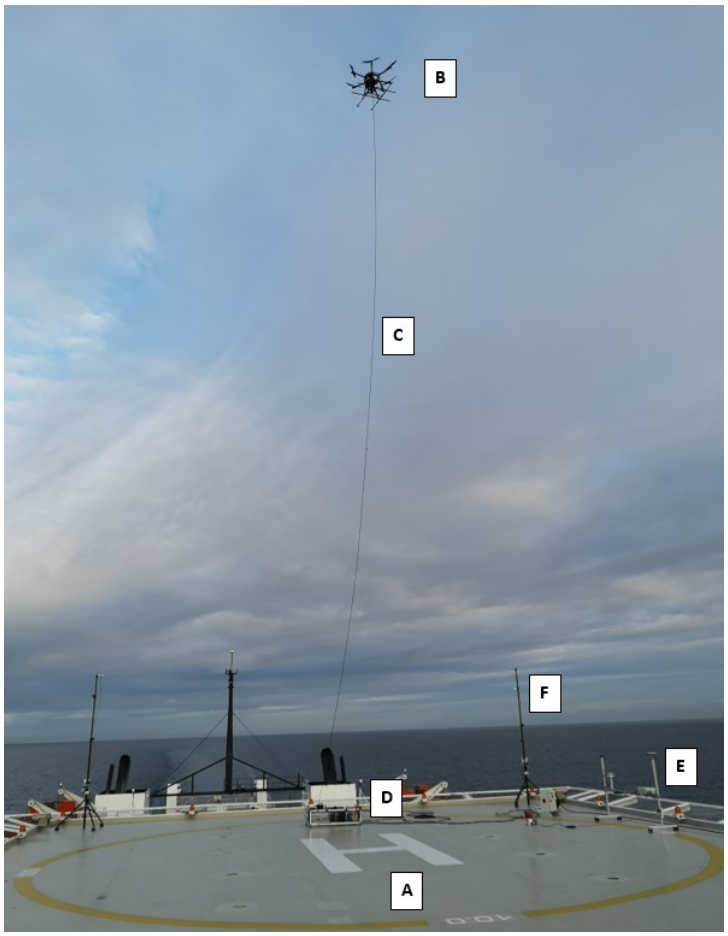

Figure 9. Tethered hexacopter during fligt tests.

In Figure 9 the ship's helipad deck (Figure 9A), the multirotor in the follow-me flight above the ship's deck (Figure 9B), the UAV power cord transmitting electricity from the vessel's deck (Figure 9C), the unwinder of the power cord (Figure 9D), the navigation station (Figure 9E) and one of the masts of the UwB local navigation system (Figure 9F) are presented.

Preprints (www.preprints.org) | NOT PEER-REVIEWED | Posted: 4 July 2023 doi:10.20944/preprints202307.0217.v1

4. Results

During the ferry cruise described above, a number of hexarotor flight tests were carried out to check the most important components of the UAV system (local control and stabilisation system, positioning system, navigation system, landing pad following system, etc.). The results of two sample tests are shown in Figures 10–19. The first presented test was to verify the operation of the tethered hexacopter system during long-term following of the landing pad and ferry in difficult weather conditions. The second trial was designed to test the quality of hexacopter altitude tracking in a simulated UAV observation altitude change scenario. Figure 10 shows the 3d hexarotor trajectory realized during the first test. The take-off and landing points as well as the climb and descent curves have been presented and could be easily noticed. The total distance covered by the hexarotor during this test was 2.26 km. The average speed over this distance was 23.5 km/h. The hexacopter trajectory but in the ENU local coordinate system is also shown in Figure 11. The estimated position of the UAV is compared with the desired trajectory. The hexarotor, despite the difficult conditions, correctly and accurately follows the desired trajectory. Additionally, take-off and landing setpoints with current values have also been marked in Figure 11. The hexarotor attitude expressed by roll, pitch and yaw angles is shown in Figure 12. The roll angle during the entire cruise was kept about 8 degrees, while the pitch angle was about -6 degrees. The yaw angle was about 150 degrees except for the take-off and landing phases when the hexarotor was close to the ship's metal deck. The ship's large metal superstructure distorted the readings of the UAV's onboard magnetometer. Linear velocities of the propeller are shown in Figure 13. These velocities were used as control signals in the landing pad tracking system. In addition, the ground speed is shown for the comparison. The hexarotor follows the desired speed values very precisely, except for the critical take-off phase caused by disturbances of the magnetometer and disturbances from gusts of wind, intensified at relatively low altitudes close to the deck (air streams are reflected from the deck surface and hit the hexarotor—the ground effect). Magnetometer readings during the test are shown in Figure 14. It is easy to see the effect of the proximity of the vessel metal deck on the operation of the magnetometer and the determination of the yaw angle.

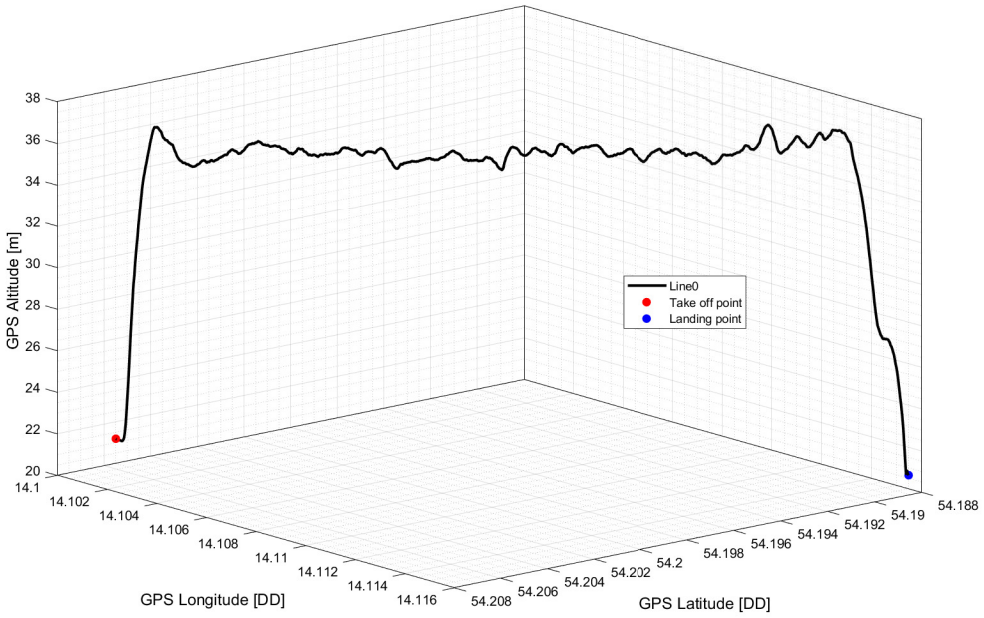

Figure 10. Tethered hexacopter trajectory (GPS) during the long-term following test.

Preprints (www.preprints.org) | NOT PEER-REVIEWED | Posted: 4 July 2023 doi:10.20944/preprints202307.0217.v1

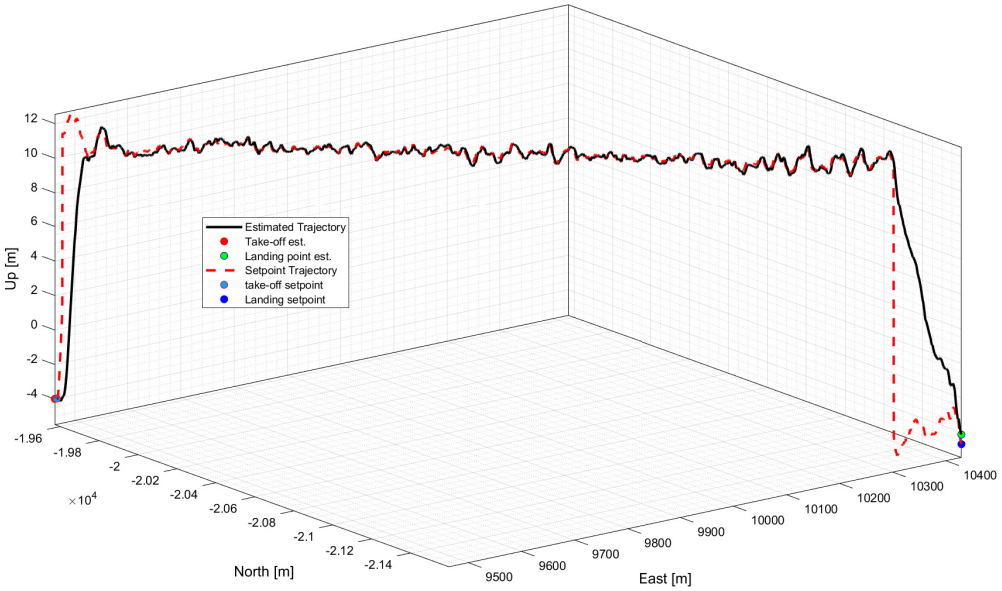

Figure 11. Tethered hexacopter trajectory (local ENU frame) during the long-term following test.

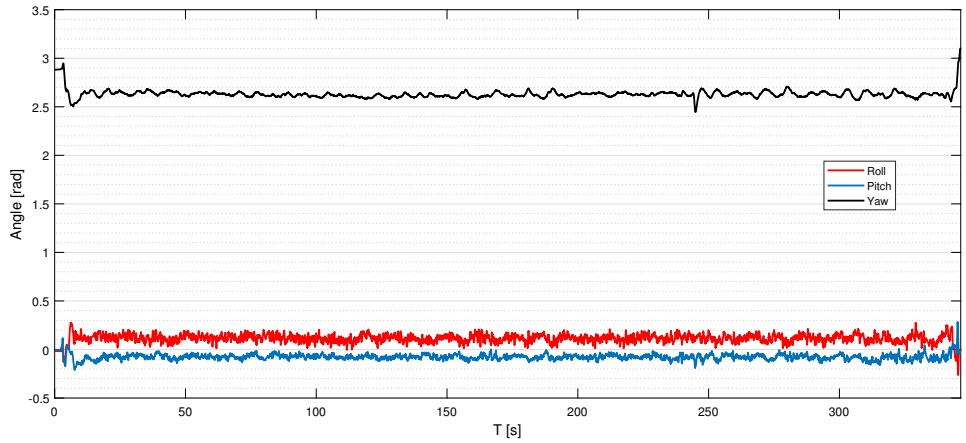

Figure 12. Tethered hexacopter attitude during the long-term following test.

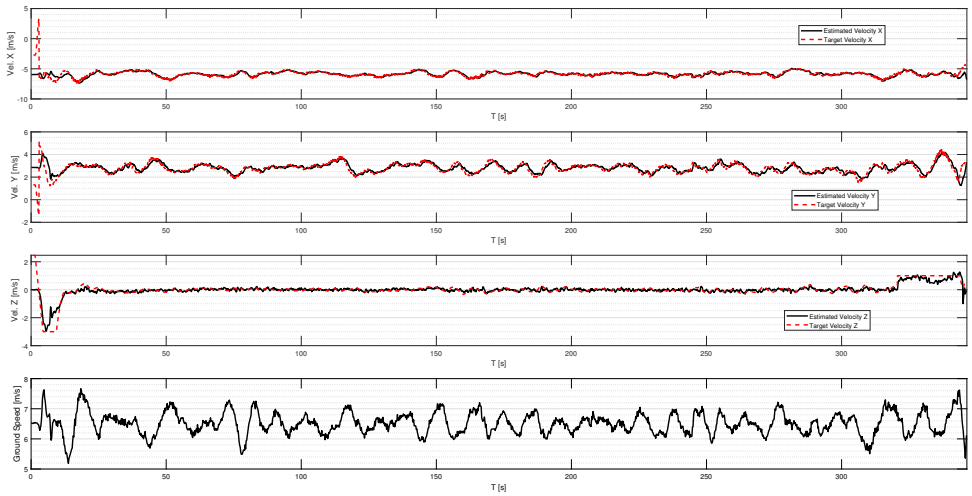

Figure 13. Tethered hexacopter linear velocities and ground speed during the long-term following test.

Preprints (www.preprints.org) | NOT PEER-REVIEWED | Posted: 4 July 2023 doi:10.20944/preprints202307.0217.v1

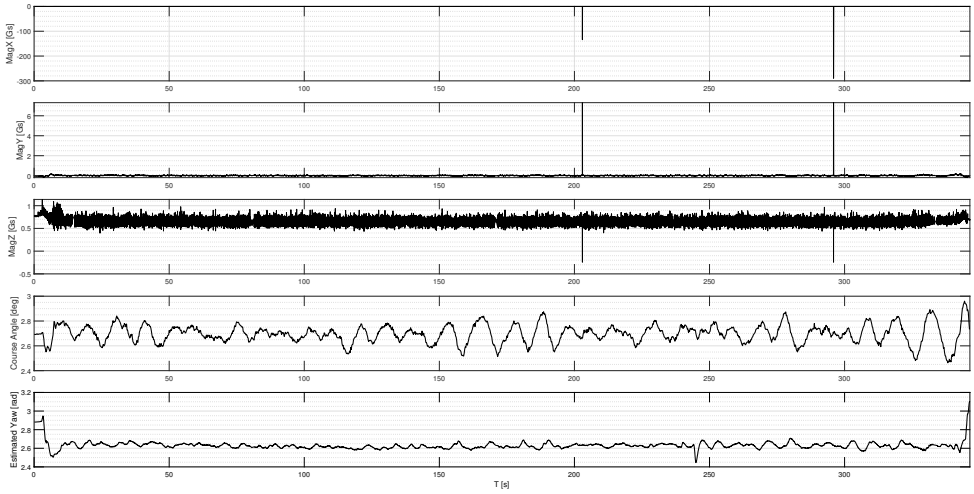

Figure 14. Tethered hexacopter magnetometer readings and course angle during the long-term following test.

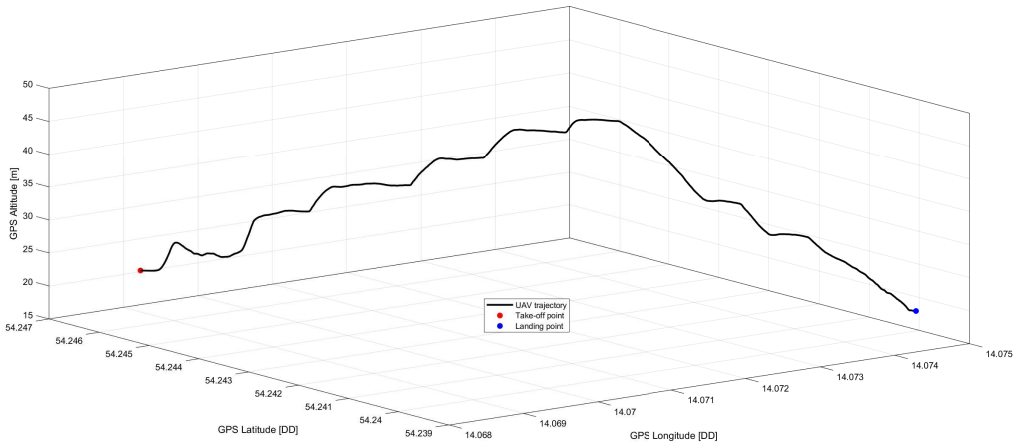

Figure 15. Tethered hexacopter trajectory (GPS) during the altitude following test.

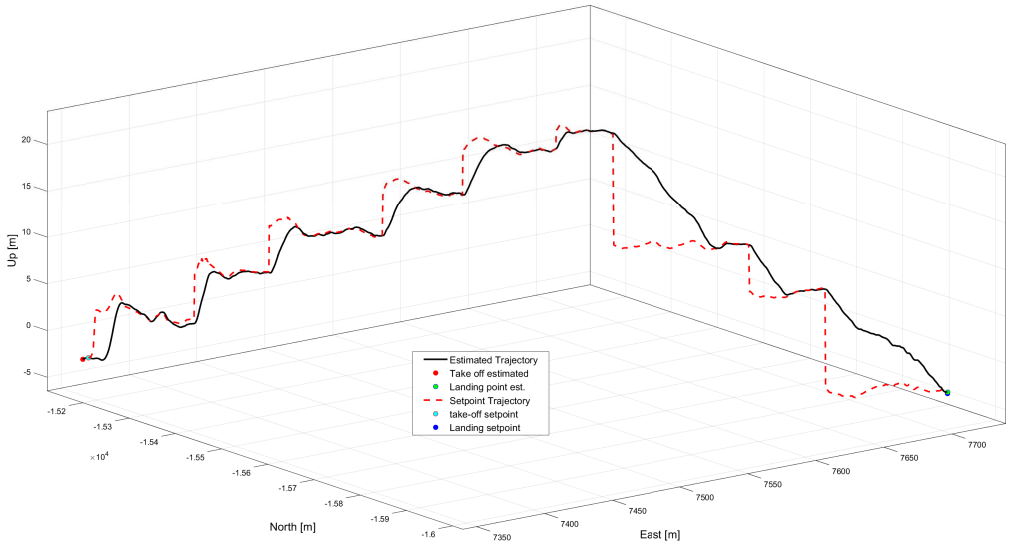

Figure 16. Tethered hexacopter trajectory (local ENU frame) during the altitude following test.

Preprints (www.preprints.org) | NOT PEER-REVIEWED | Posted: 4 July 2023 doi:10.20944/preprints202307.0217.v1

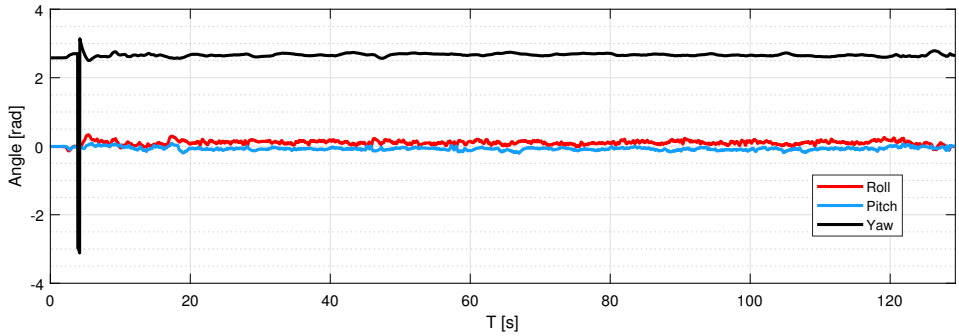

Figure 17. Tethered hexacopter attitude during the altitude following test.

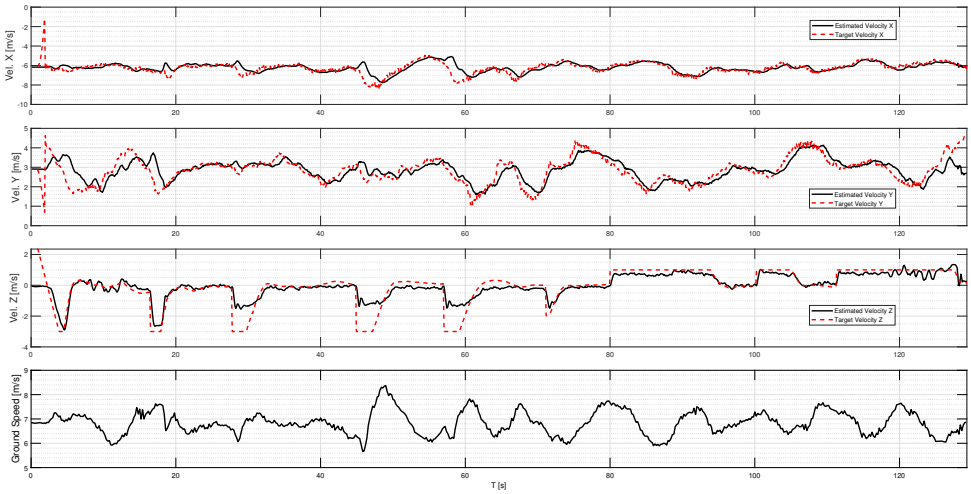

Figure 18. Tethered hexacopter linear velocities and ground speed during the altitude following test.

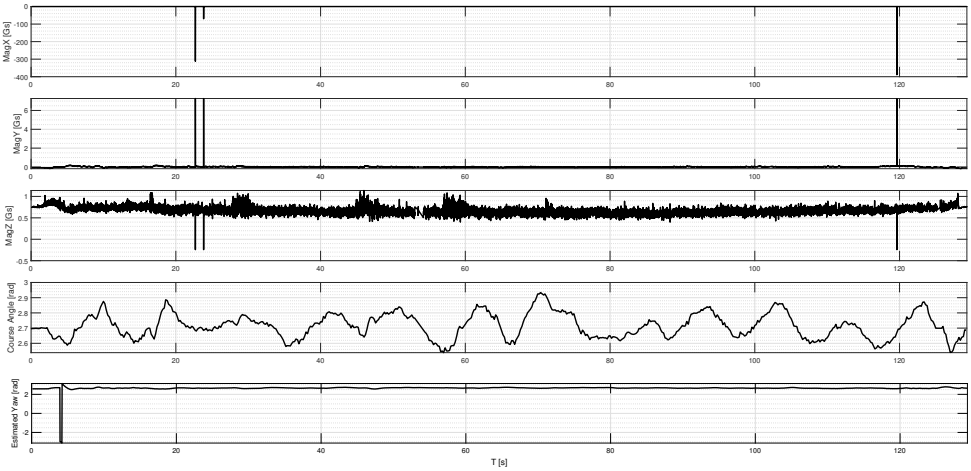

Figure 19. Tethered hexacopter magnetometer readings and course angle during the altitude following test.

The second test involved checking the hexacopter and its navigation system in an observation scenario at various altitudes in hard sea conditions. Changing the flight altitude (ascending, descending) while following the vessel in windy conditions and operating from a vessel helipad is a challenge. The vessel structure intensifies wind disturbances, gusts and numerous air chimneys

Preprints (www.preprints.org) | NOT PEER-REVIEWED | Posted: 4 July 2023 doi:10.20944/preprints202307.0217.v1

noted in the vicinity of the vessel landing pad. Similarly to the results of the first long-distance test, the UAV trajectory and the most important flight parameters are shown in Figures 15–19. In Figure 15 the hexacopter trajectory during the second test is presented. It is easy to see the changes in altitude intentionally triggered in the control system. During the second test, the hexacopter covered the distance at almost 900 m with an average speed of 25 km/h. The hexacopter trajectory in the ENU local coordinate system is also shown in Figure 16. Here, the set values of the trajectory and the estimated position in the local frame in the ENU reference system can be easily compared. It can be seen that the quality of tracking the desired trajectory, despite difficult weather and environment conditions, is satisfactory. The roll, pitch and yaw angles during the second test are shown in Figure 17. The average value of the roll angle during the test was 6 degrees, while the pitch angle was about -5 degrees. The yaw angle during the entire test was 150 degrees with a jump to $+150$ degrees in the initial phase of the test (just after the start). This is caused by large changes in the magnetic field in a close proximity to the vessel metal deck. Control system quality evaluation can also be carried out using the analysis of linear velocities (desired and measured values). They are shown in Figure 18. The control system follows the set point properly. The largest changes in the setpoint can be seen in the z-axis velocity component. This is caused by forced changes in altitude setpoint. As in the previous test, magnetometer readings are presented in Figure 19. It is easy to see the effect of the proximity of the vessel metal deck on the operation of the magnetometer and the determination of the yaw angle.

5. Conclusions

Tests in the real conditions are always the best way to verify the correctness and effectiveness of the designed systems, especially flying systems such as UAVs. Assumptions made during the design process are usually reformulated and valuable knowledge about the tested object is collected. In the case of the tested tethered hexacopter, the flights at sea during a standard "Wolin" ferry voyage made it possible to identify some exciting issues. The most important issue concerns the magnetometer readings on the ferry's landing pad. The varying drift from the real magnetic north which decreases with flight altitude increment is observed, especially on the plots of magnetometer z-axis readings just after take-off and just before landing (Figures 14 and 19). Moreover, the z-axis readings of the magnetometer are very noisy in comparison to the x and y axes. Of course, the problem source is in the structure material from which the ferry is made. Steel is a ferromagnetic material, which impacts the weak magnetic field of the Earth. The magnetometer is the most crucial device among other hexacopter onboard equipment because it is the only source of heading that is required to track the landing pad position while the ferry is cruising. At the low cruise speed of the ferry, the GNSS heading readings are unreliable. During the tests, a solution to this problem was found, which includes magnetometer recalibration before each take-off. Thus, the conclusion is that the automated process of flight management especially if it has to be done by a computer of an autonomous vessel, must include a flight preparation phase responsible for magnetometer tests and recalibration. Another important issue arises from air vortices around the landing pad, at the altitude up to 5 meters. They are made by the wind's air mass reflected by the vessel's side and other equipment located around the landing pad and the airflow related to vessel movement. In the case of the ferry, its landing pad is almost at the top of the ferry's body just behind the captain's bridge and these are ideal conditions for such vortices. Because of these vortices, the take-off phase is extremely unstable up to 5 meters above the surface of the landing pad. There is no possibility to mount wind deflectors around the landing pad, so the only way to reduce crash risk is to perform take-off with the maximum vertical speed to jump through the vortices' area. During flights performed in real maritime conditions, no significant impact of the aerodynamic drag of the power cord was observed. The unwinder always provided proper tension and the required length of the cord. The only issue was related to the winding speed while the hexacopter falled freely due to a motor fault. The winding speed was too low because it was tuned to the normal landing phase. Therefore, the emergency procedure enabling the maximum speed of the unwinder motor in the case of a fault of one of the hexacopter motors should be provided and launched

by the flight management computer. Thus, during the tests in real maritime conditions, the issues that could be critical in the implementation phase of the hexacopter, were identified. The gathered experience and knowledge will be utilized during future projects, aiming at UAV systems design for unmanned vessels. Preparing and carrying out the tests on the ferry "Wolin" landing pad was highly risky because the landing pad and the ferry's deck are not prepared for the flying UAVs. Any free fall of the tethered hexacopter is dangerous for the researchers, ferry crew, and navigation devices on the ferry deck. Thus, successful tests without any crashes must be considered a great achievement.

Author Contributions: Conceptualization, L.A., M.C., A.W. S.R., D.O., A.B., and C.K.; methodology, L.A., M.C., A.W. S.R., D.O., A.B., and C.K.; software, L.A., M.C., and A.W.; validation, L.A., M.C., A.W. S.R., D.O., and A.B.; formal analysis, L.A., M.C., A.W. S.R., D.O., and A.B.; investigation, L.A., M.C., A.W. S.R., D.O., A.B. and C. K.; resources, L.A., M.C., A.W. S.R., D.O., and A.B.; data curation, L.A., M.C., A.W. S.R., D.O., and A.B.; writing—original draft preparation, L.A., M.C., A.W. S.R., D.O., A.B., and C.K.; writing—review and editing, L.A., M.C., A.W. S.R., D.O., A.B., Z.K. and C.K.; visualization, L.A., M.C., A.W. S.R., D.O., and A.B.; supervision, C.K.; project administration, C.K.; funding acquisition, L.A., M.C., A.W. S.R., D.O., A.B., C.K. and Z.K. All authors have read and agreed to the published version of the manuscript.

Funding: This work was supported by the National Center of Research and Development, Poland, as a part of the project entitled Application research in the area of navigation, control, communication and data exchange between an autonomous vessel and an aircraft—financed by the European Regional Development Fund as a part of the Smart Growth Operational Programme 2014–2020 (POIR.04.01.04-00-0025/16). This article was also supported by statutory funds of the Department of Mechanical Engineering: WZ/WM-IIM/2/2022, and statutory funds of the Department of Electrical Engineering: WZ/WE-IA/4/2023.

Institutional Review Board Statement: Not applicable.

Informed Consent Statement: Not applicable.

Data Availability Statement: Not applicable.

Conflicts of Interest: The authors declare no conflict of interest.

References

1. Wei, L.; Tao, Z.; Shengjun, H.; Kaiwen, L. A hybrid optimization framework for UAV reconnaissance mission planning, Computers & Industrial Engineering, Volume 173, 2022, 108653, ISSN 0360-8352, https://doi.org/10.1016/j.cie.2022.108653,
2. Santos, N. P.; Rodrigues, V. B.; Pinto, A. B. and Damas B. Automatic Detection of Civilian and Military Personnel in Reconnaissance Missions using a UAV, 2023 IEEE International Conference on Autonomous Robot Systems and Competitions (ICARSC), Tomar, Portugal, 2023, pp. 157-162, doi: 10.1109/ICARSC58346.2023.10129575,
3. Ahmadian, N.; Lim, G.J.; Torabbeigi, M.; Kim, S.J. Smart border patrol using drones and wireless charging system under budget limitation, Computers & Industrial Engineering, Volume 164, 2022, 107891, ISSN 0360-8352, https://doi.org/10.1016/j.cie.2021.107891,
4. Namburu, A.; Selvaraj, P.; Mohan, S.; Ragavanantham, S.; Eldin, E.T. Forest Fire Identification in UAV Imagery Using X-MobileNet. Electronics 2023, 12, 733. https://doi.org/10.3390/electronics12030733,
5. Li, Y.; Yuan, H.; Wang, Y.; Xiao, C. GGT-YOLO: A Novel Object Detection Algorithm for Drone-Based Maritime Cruising. Drones 2022, 6, 335. https://doi.org/10.3390/drones6110335,
6. Muttin, F. Umbilical deployment modeling for tethered UAV detecting oil pollution from ship, Applied Ocean Research, Volume 33, Issue 4, 2011, Pages 332-343, ISSN 0141-1187, https://doi.org/10.1016/j.apor.2011.06.004,
7. Kownacki, Cezary.; Ambroziak, L.; Ciezkowski, M., Wolniakowski, A. Romaniuk, S.; Bożko, A.; Oldziej, D. Precision Landing Tests of Tethered Multicopter and VTOL UAV on Moving Landing Pad on a Lake. *Sensors* **2023**, *23*. https://10.3390/s23042016
8. Colomina, I.; Molina, P. Unmanned aerial systems for photogrammetry and remote sensing: A review. *ISPRS J. Photogramm. Remote Sens.* **2014**, *92*, 79–97.
9. Agrafiotis, P.; Skarlatos, D.; Georgopoulos, A.; Karantzalos, K. Shallow Water Bathymetry Mapping from UAV Imagery Based on Machine Learning. *Int. Arch. Photogramm. Remote Sens. Spat. Inf. Sci.* **2019**, *XLII-2/W10*, 9–16.

10. Burdziakowski, P. Increasing the Geometrical and Interpretation Quality of Unmanned Aerial Vehicle Photogrammetry Products Using Super-resolution Algorithms. *Remote Sens.* **2020**, *12*, 810.
11. Dhaliwal, S.S.; Ramirez-Serrano, A. Control of an unconventional VTOL UAV for search and rescue operations within confined spaces based on the Marc control architecture. In Proceedings of the 2009 IEEE International Workshop on Safety, Security Rescue Robotics (SSRR 2009), Denver, CO, USA, 3–6 November 2009; IEEE: Piscataway, NJ, USA, 2009; pp. 1–6.
12. Fabiani, P.; Fuertes, V.; Piquereau, A.; Mampey, R.; Teichteil-Königsbuch, F. Autonomous flight and navigation of VTOL UAVs: From autonomy demonstrations to out-of-sight flights. *Aerosp. Sci. Technol.* **2007**, *11*, 183–193.
13. Okulski, M.; Ławryńczuk, M. A Small UAV Optimized for Efficient Long-Range and VTOL Missions: An Experimental Tandem-Wing Quadplane Drone. *Appl. Sci.* **2022**, *12*, 7059.
14. Lewicka, O.; Specht, M.; Specht, C. Assessment of the Steering Precision of a UAV along the Flight Profiles Using a GNSS RTK Receiver. *Remote Sens.* **2022**, *14*, 6127.
15. Dąbrowski, P.S.; Specht, C.; Specht, M.; Burdziakowski, P.; Makar, A.; Lewicka, O. Integration of Multi-source Geospatial Data from GNSS Receivers, Terrestrial Laser Scanners, and Unmanned Aerial Vehicles. *Can. J. Remote Sens.* **2021**, *47*, 621–634,
16. Yang, B.; Yang, E. A Survey on Radio Frequency based Precise Localisation Technology for UAV in GPS-denied Environment. *J. Intell. Robot. Syst.* **2021**, *103*, 38.
17. Paul, H.; Miyazaki, R.; Kominami, T.; Ladig, R.; Shimonomura, K. A Versatile Aerial Manipulator Design and Realization of UAV Take-Off from a Rocking Unstable Surface. *Appl. Sci.* **2021**, *11*, 9157. https://doi.org/10.3390/app11199157.
18. Tang, H.; Zhang, D.; Gan, Z. Control System for Vertical Take-Off and Landing Vehicle's Adaptive Landing Based on Multi-Sensor Data Fusion. *Sensors* **2020**, *20*, 4411. https://doi.org/10.3390/s20164411.
19. Chang, C.-W.; Lo, L.-Y.; Cheung, H.C.; Feng, Y.; Yang, A.-S.; Wen, C.-Y.; Zhou, W. Proactive Guidance for Accurate UAV Landing on a Dynamic Platform: A Visual–Inertial Approach. *Sensors* **2022**, *22*, 404. https://doi.org/10.3390/s22010404.
20. Grlj, C.G.; Krznar, N.; Pranjić, M. A Decade of UAV Docking Stations: A Brief Overview of Mobile and Fixed Landing Platforms. *Drones* **2022**, *6*, 17. https://doi.org/10.3390/drones6010017.
21. Acevedo, J.J.; García, M.; Viguria, A.; Ramón, P.; Arrue, B.C.; Ollero, A. Autonomous Landing of a Multicopter on a Moving Platform Based on Vision Techniques. In Proceedings of the ROBOT 2017: Third Iberian Robotics Conference, ROBOT 2017, Sevilla, Spain, 22–24 November 2017; Ollero, A., Sanfeliu, A., Montano, L., Lau, N., Cardeira, C., Eds.; Advances in Intelligent Systems and Computing; Springer: Cham, Sweitzerland, 2017; Volume 694.
22. Shao, G.; Ma, Y.; Malekian, R.; Yan, X.; Li, Z. A Novel Cooperative Platform Design for Coupled USV–UAV Systems. *IEEE Trans. Ind. Inform.* **2019**, *15*, 4913–4922.
23. Narváez, E.; Ravankar, A.A.; Ravankar, A.; Emaru, T.; Kobayashi, Y. Autonomous VTOL-UAV Docking System for Heterogeneous Multirobot Team. *IEEE Trans. Instrum. Meas.* **2021**, *70*, 5500718.
24. Palafox, P.R.; Garzón, M.; Valente, J.; Roldán, J.J.; Barrientos, A. Robust Visual-Aided Autonomous Takeoff, Tracking, and Landing of a Small UAV on a Moving Landing Platform for Life-Long Operation. *Appl. Sci.* **2019**, *9*, 2661. https://doi.org/10.3390/app9132661.
25. Alarcón, F.; García, M.; Maza, I.; Viguria, A.; Ollero, A. A Precise and GNSS-Free Landing System on Moving Platforms for Rotary-Wing UAVs. *Sensors* **2019**, *19*, 886. https://doi.org/10.3390/s19040886.
26. Aissi, M.; Moumen, Y.; Berrich, J.; Bouchentouf, T.; Bourhaleb, M.; Rahmoun, M. Autonomous solar USV with an automated launch and recovery system for UAV: State of the art and Design. In Proceedings of the 2020 IEEE 2nd International Conference on Electronics, Control, Optimization and Computer Science (ICECOCS), Kenitra, Morocco, 2–3 December 2020; pp. 1–6.
27. Kontron. *pITX-E38, ULTRASMALL 2.5 " Pico-ITX BOARD WITH Intel® Atom™ E38XX*; Kontron: Augsburg, Germany, 2016.
28. U-blox. *NEO-M8P u-blox M8 High Precision GNSS Modules*; No. UBX-15016656; u-blox: Thalwil, Switzerland, 2020.
29. Sparton. *AHRS-8, Attitude Heading Reference System*; No. 12.21.17; Sparton: Schaumburg, IL, USA, 2017.
30. PX4 Autopilot User Guide (main). Available online: hhttps://docs.px4.io/main/en/ (accessed on 29 May 2023).

31. PX4 Controller Diagrams. Available online: https://docs.px4.io/main/en/flight_stack/controller_diagrams.html (accessed on 29 May 2023).
32. Barral, V.; Escudero, C. J.; García-Naya, J. A. NLOS Classification Based on RSS and Ranging Statistics Obtained from Low-Cost UWB Devices. In Proceedings of the 27th European Signal Processing Conference (EUSIPCO), A Coruna, Spain, 2–6 September 2019; pp. 1–5. https://doi.org/10.23919/EUSIPCO.2019.8902949.
33. Janczak, D.; Walendziuk, W.; Sadowski, M.; Zankiewicz, A.; Konopko, K.; Idzkowski, A. Accuracy Analysis of the Indoor Location System Based on Bluetooth Low-Energy RSSI Measurements. *Energies* **2022**, *15*, 8832. https://doi.org/10.3390/en15238832.